

## Article

# Architectural, Constructional and Structural Aspects of a Historic School in Greece. The Case of the Elementary School in Arnaia, Chalkidiki

Vasiliki Pachta <sup>1,\*</sup>, Vasiliki Terzi <sup>2,†</sup>  and Evangeliki Malandri <sup>1</sup>

<sup>1</sup> Lab. of Building Materials, School of Civil Engineering, Aristotle University of Thessaloniki, 54124 Thessaloniki, Greece

<sup>2</sup> Institute of Statics and Dynamics, School of Civil Engineering, Aristotle University of Thessaloniki, 54124 Thessaloniki, Greece; terziv@civil.auth.gr (V.T.); evmaland@civil.auth.gr (E.M.)

\* Correspondence: vpachta@civil.auth.gr; Tel.: +30-2310995882

† These authors contributed equally to this work.

**Abstract:** Historic school buildings were built during the end of the 19th century and into the beginning of the 20th century, using the traditional and locally available building materials and techniques, and most of them still function as schools. Because of the requirements arising from their constant use, there is an intense interest in their structural and energy integration, while there is limited research on the tangible and intangible values they encompass. In this study, an effort has been made to assess the historical, architectural, constructional and structural aspects of a historic school building located in the town of Arnaia, in the mountainous part of Chalkidiki peninsula, Northern Greece. The study included on-site inspection, architectural overview, determination and mapping of the constructional materials and techniques applied, as well as investigation of the preservation state of the building. Additionally, a structural analysis of the system was performed through a three-dimensional finite element model. All research data was comparatively evaluated, in order to identify the principles governing its physiognomy and structure. The objective of the study was therefore to analyze the significance and technological aspects of this unrecognized part of the common European built heritage that should be further assessed and acknowledged as a heritage asset.

**Keywords:** historic schools; built heritage; masonry; structural analysis; on-site inspection; mapping



**Citation:** Pachta, V.; Terzi, V.; Malandri, E. Architectural, Constructional and Structural Aspects of a Historic School in Greece. The Case of the Elementary School in Arnaia, Chalkidiki. *Heritage* **2021**, *4*, 1–19. <https://doi.org/10.3390/heritage4010001>

Received: 1 December 2020

Accepted: 22 December 2020

Published: 26 December 2020

**Publisher's Note:** MDPI stays neutral with regard to jurisdictional claims in published maps and institutional affiliations.



**Copyright:** © 2020 by the authors. Licensee MDPI, Basel, Switzerland. This article is an open access article distributed under the terms and conditions of the Creative Commons Attribution (CC BY) license (<https://creativecommons.org/licenses/by/4.0/>).

## 1. Introduction

Historic schools built during the end of the 19th and into the beginning of the 20th century concern a significant part of the common European built heritage, which is not however adequately acknowledged [1–4]. Their individual characteristics and evolution can be related to multiple parameters concerning the wider historical and socioeconomic aspects of each region, the educational policies applied, as well as the regional principles of construction [3–6]. Nowadays, they still function for educational or secondary purposes and in many cases they have been abandoned or even demolished [6–11].

The buildings erected around the Mediterranean basin (Greece, Italy, France, Spain) present various structural similarities, since their construction was governed by the principle of functionality [3–7]. Their architectural characteristics varied, according to the style adopted (traditional, Eclecticism, Neoclassicism), while the organization of the inner spaces was reflected in the façades [2,7,8,10]. They were usually built according to locally available building materials and techniques, as well as to the technological background of each region. From the 19th century on, specific guidelines for the construction of school buildings were constituted, according to the educational needs and priorities of each state [9,12,13].

Generally, the structural integrity and energy efficiency of these constructions were the primary goals, since they hosted numerous students of all levels. The floor plans

were usually symmetrically arranged, following a successive placement of the classrooms around or alongside a main corridor [1,2,6,7]. In order to achieve natural ventilation and lighting, the orientation of the building, as well as the dimensions, typology and organization of the openings, played an important role [1,2,6,14–16].

The abovementioned characteristics can be found in relevant studies given in literature, concerning a limited era of 50–70 years [6–11]. For example, a studied school building in Spain [6], dating from 1927 and still functioning as an elementary school, comprised a two-storey stone masonry structure with a C-shaped ground plan. The orientation was south–west and the large, arched openings were symmetrically organized in the façades. The inner spaces (classrooms) were also symmetrically arranged around a central corridor, both on the ground and first floors, while the external walls were rendered and 60 cm thick. Historic school buildings in Italy [7,10], erected during the beginning of the 20th century, comprised rectangular stone masonry buildings (two to three storeys), also with symmetrically arranged openings. In Algeria, on the other hand, a school building dating from 1874 [11], comprised a stone masonry structure (wall thickness 50–60 cm), consisting of four floors (basement, ground, 1st, and 2nd floors). The ground plan was  $\Pi$ -shaped, with a successive arrangement of the classrooms alongside the main corridor and symmetrically organized large openings (1 m  $\times$  2m).

In Greece, education was a significant part of cultural life, even from the ancient times [13], while the educational policies applied were closely related to the wider historical and social aspects of each era and region [17,18]. Until the end of the 18th century, school activities were hosted in private houses or religious buildings (monasteries, churches), with education closely related to religion [17]. The first school buildings started to be erected at the end of the 18th century and were neighboring to religious buildings or remote from the settlements in order to achieve isolation (according to the monastic principles) [17,19]. Their construction was systemized at the beginning of the 19th century, under the responsibility of the Greek State [17,20,21].

The building types evolved around one central and gradually more classrooms, successively arranged alongside a main corridor [20–22]. The ground plan was mainly rectangular and symmetrically organized, while dimensions varied according to the regional educational needs [17,20,21]. The first national program of school buildings was legislated in 1894 [23] and was reformed in 1929 [17,24]. During the period 1928–1932, more than 3000 schools were erected [17], following the traditional and contemporary principles of construction.

Nowadays, there is an intense interest in the study of historic school buildings, mainly focusing on their energy efficiency [5,6,11,14] and structural integrity [1,7,10], since most of them are still in use. However, there is limited research on the tangible and intangible values they incorporate, although in some cases they have been listed and identified as cultural assets. To this end, their constructional and technological characteristics should be further assessed, as well as their historical, educational and architectural values.

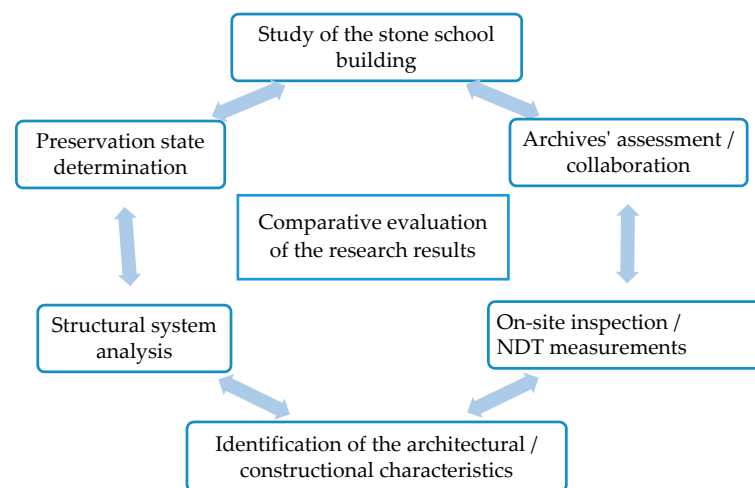
In this paper, an effort has been made to study the historic school building located in Arnaia, Chalkidiki peninsula, Northern Greece. The building was erected in 1928, is still functioning as an elementary school, and comprises three floors (semi-basement, elevated ground floor, 1st floor). It comprises a mixed-type structure consisting of unreinforced stone masonry and reinforced concrete elements (slabs, beams). The study aimed to identify the historical, architectural and constructional aspects of the building, as well as to assess its structural integrity and preservation state. The results were comparatively evaluated in order to document the principles governing its construction.

The objective of the study was to analyze the significance and technological aspects of this unrecognized part of the common European built heritage, which should be further assessed and acknowledged as a heritage asset. Due to their permanent use and extensive needs for maintenance, or even to the inadequacy of the relevant sectors responsible for their use, historic school buildings are constantly subjected to repair work, often contradictory to the principles of restoration. Therefore, it is important to redefine the

cultural identity of these structures, taking into account the wider and individual values they encompass and preserving them for the future generations. Since there are several constructional similarities in this type of building, this study can also serve as a source of information for future research.

## 2. Methodology

In order to study the elementary school of Arnaia, a specific methodology was followed [24–26], as presented in Scheme 1. It firstly comprised of an assessment of historic archives, educational material, existing architectural designs and technical reports provided by all relevant sectors. To this end, a close collaboration with the Aristotle Municipality (responsible for the regional school buildings) and the directorate of elementary education of Chalkidiki was implemented. Additionally, the director of the school, the architects involved in a past restoration study of the building, as well as citizens of the settlement, provided valuable information.



**Scheme 1.** Schematic flowchart of the methodology followed during the study.

The second stage concerned a detailed on-site inspection of the building. It included a thorough photographic documentation, identification of the main architectural and constructional aspects, as well as documentation of the building materials and techniques confronted [24–26]. To achieve this, nondestructive techniques were applied, including Schmidt hammer rebound tests for estimating the materials’ strength and profometer measurements for the detection of reinforcement in the concrete elements [26–28]. The latter were implemented in various locations of the building, and in each location multiple values were recorded (4–6). Schmidt hammer testing was performed on the concrete slabs of the ground to the 1st floor, as well as on the masonries (external, internal) of the structure.

Since the structure was mixed type, including unreinforced masonry and reinforced concrete elements, it was significant to investigate the type and location of the building materials, as well as the constructional techniques applied. To this extent, a plan of the ground and the 1st floor was conducted in order to further assess the exact mapping of the building materials.

The preservation state of the building was also identified, regarding the detection of the pathology symptoms and damages encountered. Additionally, an analysis of the structural system was assessed through a three-dimensional finite element model of the structure. The main targets were: (i) detailed representation of the structural geometry; (ii) estimation of the mechanical characteristics of the materials; (iii) definition of the loading combinations for ultimate limit state design situations; (iv) conduction of static, modal and dynamic spectral analyses.

All information and results were comparatively evaluated in order to define the architectural, constructional and structural aspects of the historic school building, with regard to its historical background and the diachronic functional requirements of its use.

### 3. Results and Discussion

#### 3.1. Geographical and Historical Background

The studied school building is located in the town of Arnaia, situated in the northeastern (mountainous) part of Chalkidiki peninsula, in Northern Greece (Figure 1a). The town belongs to the Aristotle Municipality (consisting of 15 settlements) and has been inhabited since ancient times. It was amphitheatrically built in a mountainous area (600m altitude) with unique landscapes, fauna and flora, while it is distinguished for the preservation of its traditional customs and architecture. There is a great stock of stone masonry buildings dating from the end of the 19th to the beginning of the 20th century, most of which have been restored, depicting the regional traditional building technology.



**Figure 1.** Geographical location of Arnaia and its historic schools (Google maps). (a) Arnaia; (b) the location of the Municipality building (1871) and of the elementary school (1928).

According to the survey, there are two historic school buildings in Arnaia (Figure 1b). The first one (Figure 2a), was constructed in 1871 and is the oldest school of the region. It was built in the center of the settlement, next to the church of S. Stefanos and attached to its tower bell (built later during 1884) (Figure 2b). The building, comprising two storeys, has a rectangular plan and was built with stone masonry. It functioned as an elementary school until the year 1935, then as a high school (1936–1940), and later as a storehouse. Due to the severe damages it experienced, it was decided to demolish it in 1970. The citizens and church made great efforts to cancel the demolition works (resulting in the destruction of the roof and of the internal walls) and preserve it. In 1980 it was listed as a monument and was completely restored, in order to host the municipality's authorities.



**Figure 2.** The historic school building of Arnaia (1871), now hosting the municipality's authorities: (a) Main façade (SW); (b) back side (NE).

The second historic school building of the settlement, which is the case of this study, was built in 1928 and started functioning as an elementary school in 1931. From the correlation of the contemporary state (Figure 3a) with the historic photograph of 1931 (Figure 3b), it was generally asserted that the structure of the building was maintained throughout its service life. The whitish serrated frames of the openings (described later) prevailed in the façades, while the masonry was initially unrendered throughout the whole height. Additionally, access to the ground floor was initially made by a wooden staircase (Figure 3b), which was afterwards replaced by a concrete one.



**Figure 3.** The elementary school of Arnaia (1928): (a) Main façade (S); (b) main façade (S), in a historic photo of 1931 (before the earthquake); (c) the school building in the early 1940s (after the earthquake); (d) the school building in 1984 (during a local festival).

During the earthquake of 1932 (~7 Richter), which resulted in extreme catastrophes throughout the whole area [29], the building experienced severe damages. According to the information given by the director of the school (no relevant research data was found), the damages were more intense in the 1st floor and the SE part of the building. They mostly concerned cracks in the masonry walls and render detachments that were immediately repaired (the school continued to function in the same year). As presented in Figure 3c (taken some years after the earthquake), the frames of the 1st floor openings were removed (probably due to detachments), as well as the large inscription on the roof.

During World War II the building was converted into a military storehouse, with lessons being held in private houses. During 1950–1960 extensive repair work took place, including the addition of a concrete slab in the SE part of the building (damaged during the earthquake), while in 1982 the façades were restored as well as the roof. As presented in Figure 3d (taken in 1984), the whole building was rendered with a whitish mortar layer, while the opening frames of the ground floor (probably due to deterioration) were removed.

Successive repair work took place later as well as an effort to ward energy integration (2012–2015). The opening frames were replaced on both the ground and 1st floor, while the 1st floor was externally rendered with a yellowish mortar layer. Nowadays the building still functions as an elementary school, with 12 classes of the six grades (capacity ~200 students), diachronically hosting children from neighboring villages.

### 3.2. Architectural Aspects

The building is freely located on the back side of a trapezoid plot (total area: 7200m<sup>2</sup>), situated in the eastern part of the settlement (in front of the main road). It has a rectangular plan of dimensions 42.5 m × 12m and southern orientation. The total height (from the

ground level of the S façade) is around 12m (semi-basement: 1m, ground floor: 4.6m, 1st floor: 4.4m, roof: 1.8m) (Figures 3a and 4). The internal height of the floors is 2.65m in the basement, 4.4m on the ground floor and 4.35 m on the 1st floor. The main entrance, covered with a gallery, is centrally located in the S façade and access is achieved by a large concrete staircase, constructed during the earthquake repair work (Figure 3a). A second entrance was symmetrically installed in the N façade (Figure 4a). Access to the basement is made by three independent doors on the W and E sides (Figure 4b,c).



**Figure 4.** The elementary school building of Arnaia (1928). (a) N façade; (b) E façade; (c) W façade.

The educational use of the building is mainly implemented on the ground and 1st floors, where the classrooms are located. In the basement, auxiliary spaces were recorded, comprising storage spaces (for equipment, archives and mechanical installations), toilets and an area for fitness and leisure (recently developed). Additionally, there was a kitchen installation functioning in the past for the students' meals.

As presented in Figure 5, the plans of the ground and 1st floors are simple and almost identical. The ground plan is rectangular, extended to E–W axes. There is a central projection, in the S and N (wider) side of the building, forming a semi-cruciform shape.

The inner spaces are symmetrically organized around the elongated and transversal corridor (forming a central cruciform), which symmetrically divides the plan in three parts (Figure 5). These concern the western (with the classrooms, staircase and part of the elongated corridor), the eastern (classrooms and part of the elongated corridor) and the central part, consisting of the transversal corridor that connects the S and N entrances. Classrooms have been successively developed on its both sides, while on the eastern and western parts of the ground floor there are offices. The staircase, leading to the 1st floor, is located in the back side of the building, where there is a secondary staircase with access to the basement.

The simplicity and ternary arrangement of the ground plans are also reflected in the façades. The central projections are further emphasized with white serrated frames, extended throughout the whole height. The height division in the storeys is further depicted in the façades through perimetric horizontal bands running the length of the building shell. The yellowish rendering of the 1st floor nowadays emphasizes this division; however, as it was noted, the building (except for the external walls of the semi-basement) initially remained unrendered.

The openings were symmetrically put in the façades (in equal distances), following the inner spaces' organization. They are large, with dimensions of 1.15 m × 2.8 m (b×h) and slightly arched, while externally they are perimetrically decorated with the same white serrated frame (Figure 6a).

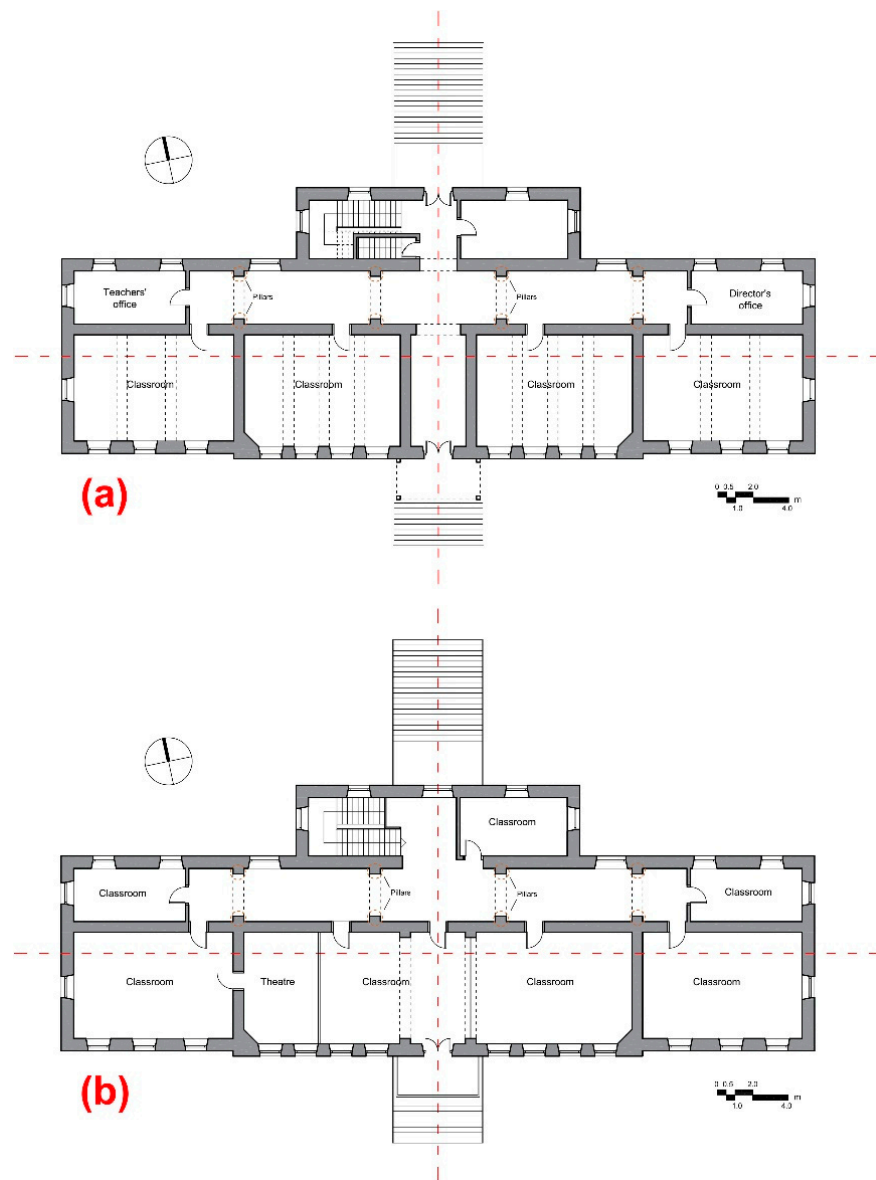


**Figure 5.** The ground plans of the elementary school of Arnaia: (a) Ground floor; (b) 1st floor.



**Figure 6.** Constructional aspects of the stone school building: (a) Opening type; (b) pillars and concrete slab of the ground floor (corridor view); (c) pillars and wooden floor of the 1st floor (corridor view); (d) inner staircase.

### 3.3. Constructional Aspects

The external and internal walls of the building comprise unreinforced stone masonry. The thickness of the walls is reduced toward the height, with the external walls varying from 85 cm (basement) to 77 cm (ground floor) and 65 cm (1st floor). Respectively, the thickness of the inner walls ranges from 75–80 cm (basement), to 65–70 cm (ground floor) and 55–60 cm (1st floor). The decrease in the wall thickness, along with the height of the building, has also been documented in many monuments and historic buildings [24–26] and could be related with the demand of reducing the construction overloads.

On the northern (external) and central (inner) elongated wall, as depicted in Figure 5, there are pillars (thickness 55–68 cm) that were put alongside the building at almost equal distances (6.5–7.0 m). They extend from the basement to the 1st floor, supporting the beams (Figure 6b,c). On the southern part of the building the beams are supported in the external and internal walls.

The masonry consists of semi-ashlar stones of local origin (limestone, sandstone, gneiss) of varying dimensions (10–20 cm × 20–40 cm). The joints of the unrendered external masonry are probably cement-based, due to the successive repair work that has taken place, while it is assumed that the initial mortars were lime-based [24,25,30]. In order to document the exact consistency of building materials, respective sampling and analysis has to be implemented. Concerning the renders and plasters of the building, these are also probably cement-based, due to subsequent repair work. Authentic plasters were recorded in the external walls of the basement, comprising a lime-based, double layer mortar (total thickness 2 cm).

Regarding the reinforced concrete elements of the construction, the profometer measurements gave valuable information (Figure 7a). From the comparative evaluation of the on-site inspection and the test results, it was concluded that reinforced concrete was used for the partial construction of the floor slabs and the staircases (Figure 6d). The concrete slab of the ground floor was extended in the corridors and was covered with the typical cement mosaic of this period. The reinforcement comprised a 24 cm × 24 cm mesh, as identified by the profometer (Figure 7a). In the eastern part of the building, a secondary reinforced concrete slab was recorded (below the wooden floor) that was put in lower than the central slab level (around 15 cm). This (according to oral testimony) was constructed during the repair works of 1950–1960, in order to further assess the damages due to the earthquake. The southern part of the building, where the classrooms are located has a wooden floor, supported by wooden beams.

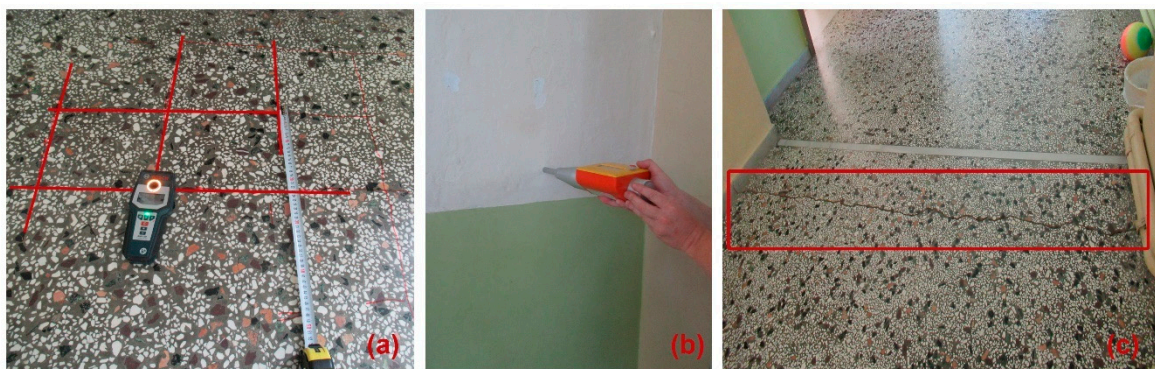


**Figure 7.** Non-destructive testing implemented and pathology symptoms. (a) Profometer measurements in the ground floor concrete slab (corridor) indicating the type and dimensions of the reinforcement; (b) Schmidt hammer tests on the external walls of the ground floor; (c) Horizontal crack in the concrete slab of the ground floor (elongate corridor, alongside the pillars).

On the 1st floor, the concrete slab was only extended in the northern part, while the rest of the floor is wooden, supported by wooden beams. Below the floor (ceiling of the ground floor) there is a wooden cover, painted with bluish color (probably authentic), while

there are successive beams (probably of R/C) supported in the masonry pillars and the central wall (Figure 6b).

The mapping of the building materials identified on the ground and the 1st floor is schematically presented in Figure 8. In these designs there is information on both the types of the floors and their coverings.

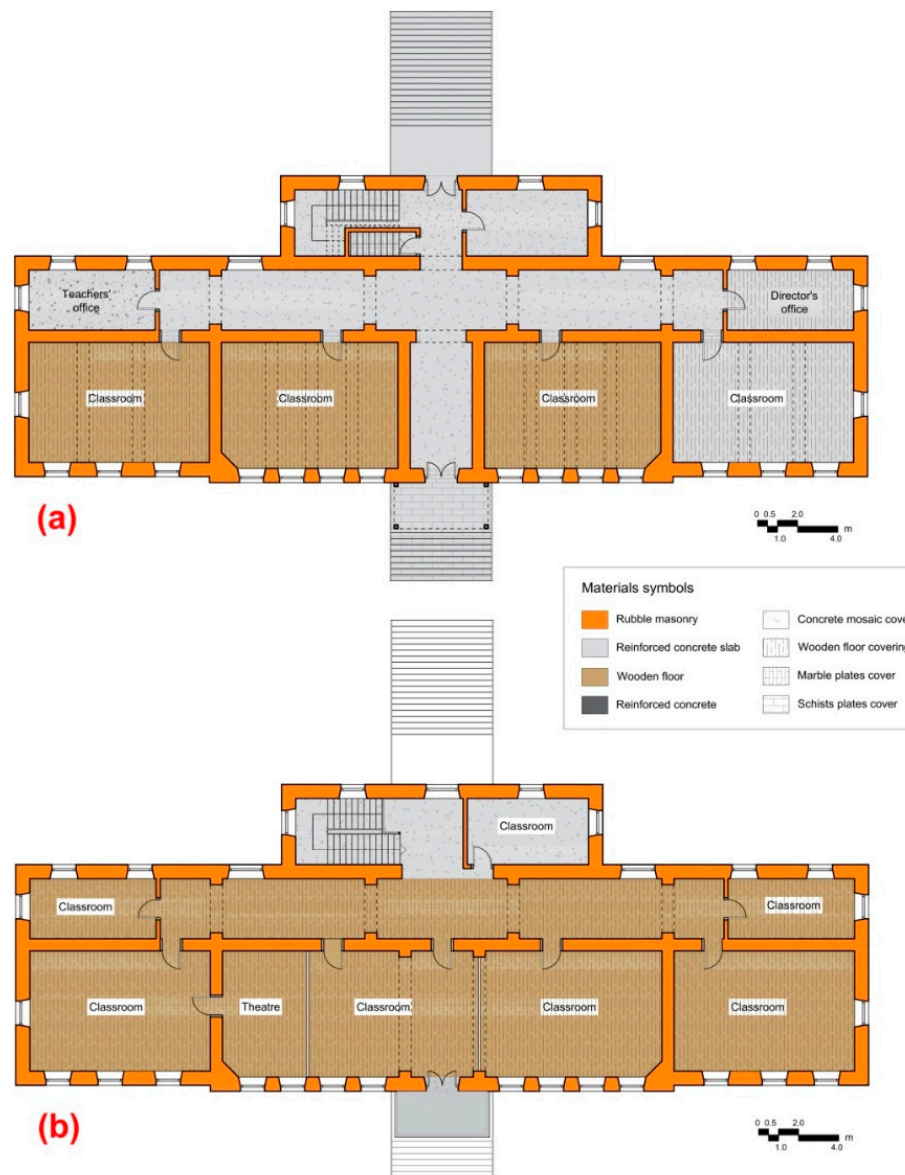


**Figure 8.** Mapping of the constructional types and materials of the stone school building: (a) Ground floor; (b) 1st floor.

According to the measurements attained by the Schmidt hammer on the various sides and constructional types of the building (Figure 7b), it was concluded that there was a relative range of values (Table 1). This was probably due to the types of the building materials, as well as to their state of preservation. The high estimated compressive strength values have also been noted in the literature [26,27] and should be verified by laboratory testing. Generally, this method can provide valuable comparable results related to the type and state of materials that should be further assessed.

The equivalent strength level of materials was envisaged (Table 1) following the equipment chart and the provisions given by ACI 228.1R-03 [31]. The stones of the masonry showed a high strength level (36–44MPa), depicting their good preservation state, while

renders and plasters had a strength of <8MPa. The strength of the R/C slabs was estimated around 28–36MPa, which was, however, extremely high and mostly related to the strength of the cement mosaic covering. This assumption could be attested to by the extensively lower strength level (10–13MPa) of the lateral side of the R/C staircase that had no covering. Nevertheless, according to ACI 228.1R-03 [31], the rebound test values are mainly affected by the surface concrete layer, without fully representing the inner structure.

**Table 1.** Schmidt hammer rebound testing measurements and estimation of compressive strength.

Structural Element	Level	Schmidt Hammer Values	Compressive Strength Estimation * [MPa]
Masonry (renders-plasters)	Basement	10–14	<8
	Ground floor	12–16	<8
	1st floor	10–20	<8
External masonry (stones)	Basement	44–50	38–44
	Ground floor	45–50	36–44
	Ground floor	40–45	28–36
R/C slab	1st floor	40–45	28–36
	-	40–45	28–36
R/C staircase (with mosaic)	-	20–24	10–13

\* The strength estimation was attained following the equipment chart and the provisions given by ACI 228.1R-03 [31].

Therefore, it was asserted that the strength level of the concrete slab was much lower than the indication given by the Schmidt hammer test and around 10–14MPa. This should be further confirmed by coring samples and strength determination through laboratory testing.

The state of the building was generally in good condition. Few damages were recorded, mainly concerning detachments of renders near to the ground level and horizontal cracks recorded in the R/C slab of the ground floor. These cracks had a range of 0.2–1 cm, were mostly identified alongside the pillars (above the beams) (Figure 7c) and should be further recorded.

### 3.4. Structural Assessment

#### 3.4.1. Finite Element Model

The structural behavior of masonry buildings can be effectively investigated via the finite element method [32], representing in detail the stiffness, self-weight, mass, and the entire set of structural elements [33–35]. The consistency between the real and the finite element geometry, concerning the openings and the wall thickness, is considered to be vital [35,36]. Along these lines, the finite element model was constructed taking into account the architectural and constructional aspects of the building, as well as the on-site inspection data. The masonry walls and plates (wooden or R/C) were modeled by the use of four node shell elements, while R/C beams were modeled by the use of two node frame elements.

Table 2 presents the geometrical and material characteristics of the main structural elements that were taken into account. All data were obtained via the on-site inspection and NDT measurements, as well as through bibliographical references [37,38].

**Table 2.** Geometrical and material characteristics of the structural elements.

Element	Thickness [m]	Modulus of Elasticity [GPa]	Weight Per Unit Volume [kN/m <sup>3</sup> ]	Poisson's Ratio [-]
Masonry	Basement	0.85	4.489	0.2
	Ground floor	0.77		
	1st floor	0.55		
R/C beams	Basement	0.6 × 0.40	26	0.2
	Ground and 1st floor	0.6 × 0.30		
R/C plate	0.2	26	25	0.25
Wooden plate	0.23	6	8	0.2

EN 1996 [39] was implemented as a main tool for the estimation of the masonry characteristic strengths. In particular, the characteristic compressive strength of the masonry received the value of  $f_k = 4.489$  MPa. The characteristic shear strength of the masonry was estimated by the equation:

$$f_{wk} = f_{vko} + 0.40 \cdot \sigma_d \quad (1)$$

where  $f_{vko}$  is the characteristic initial shear strength of the masonry, under zero compressive stress ( $f_{vko} = 0.10$  MPa), and  $\sigma_d$  is the design compressive stress.

The characteristic flexural strength, having the plane of failure parallel to the bed joints, received the value of  $f_{x1k} = 0.05$  MPa, whereas the perpendicular to the bed joints was  $f_{x2k} = 0.20$  MPa.

The basic modeling assumptions were the following: (i) use of the linear elastic material law for all the structural and non-structural elements, such as pipe work, partitions, suspended roofs, equipment, furniture [40]. Taking into account that non-structural elements may cause casualties during a seismic event and they usually define monetary losses, they must be taken into account in a retrofiting strategy [7]. However, in this preliminary stage of analysis non-structural elements were considered only in the form of permanent loading; (ii) walls and plates were modeled along their middle surface, without taking into account geometrical eccentricities; (iii) beams were modeled along their axis; (iv) the entire structure was considered to be fixed at its base and no soil–structure interaction effects were taken into account. The six degrees of freedom at the base nodes of all vertical elements were restrained; (v) the wooden roof was not included in the finite element model. The actions due to the self-weight of the roof; snow and wind were imposed as a uniform gravity loading on the top of the masonry walls located at the perimeter of the first floor; (vi) the reinforced concrete ladders were not included in the finite element model, based on outcomes of a preliminary analysis. However, the permanent and variable loads were implemented on their supports on the adjoining vertical and horizontal structural elements, in order to investigate a potential shear failure [7]. Assumptions (v) and (vi) usually referred to the case of structural parts that presented modeling peculiarities or when a more rigorous analysis of the remaining structural part was needed [33,41].

Figure 9 depicts the same basic aspects of the finite element model, according to SAP 2000 [42].

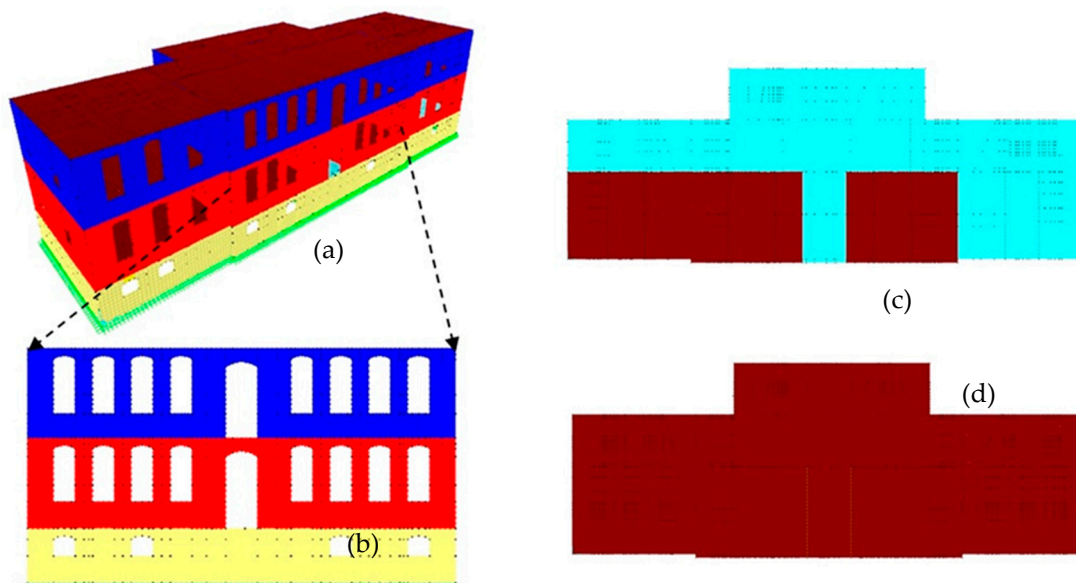


**Figure 9.** Finite element of the masonry structure [41]: (a) 3D view; (b) detailed representation of the openings; (c) horizontal elements of different materials (wooden and R/C plates); (d) wooden horizontal elements.

The stiffness of the horizontal elements depends on their modulus of elasticity, thickness (Table 2) and boundary conditions, which correspond to simple supports at their perimetric boundaries.

Modal analysis reveals information about the dynamic characteristics of a structure, while it is essential for the implementation of the dynamic spectral analysis or response-spectrum analysis; its results can be used as comparison index of performance between different numerical models [43]. According to EN 1990 [39], the mass contribution for the modal analysis is attributed to the loading combination: G+O.6Q. The number of eigenmodes calculated reached 140. The mass participation ratio at the X axis equaled 79.736% while at the Y axis it was 84.398%.

Figure 10 depicts the first three eigenmodes of the masonry building. The fundamental eigenmode corresponded to translation at the Y axis, which was perpendicular to the elongated axis, and the translational mass participation ratio at the same axis was 52.705%. The second eigenmode corresponded to torsion, rotation around the Z axis, and the mass moment of inertia participation ratio around the same axis was 48.267%. The third eigenmode corresponded to translation at the X axis, which was the elongated axis of the structure, and the translational mass participation ratio at the same axis was 63.913%.

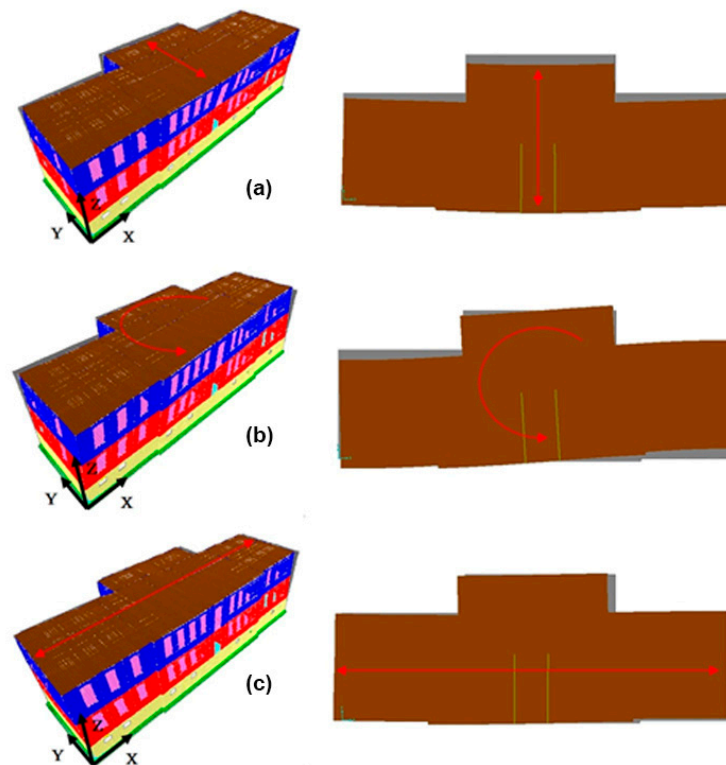


**Figure 10.** The first three eigenmodes of the masonry structure: (a) 1st eigenmode, translation at Y axis,  $T_1 = 0.184$  s; (b) 2nd eigenmode, torsion,  $T_2 = 0.154$  s; (c) 3rd, translation at X axis,  $T_3 = 0.121$  s.

The torsional mode was attributed to the distribution of the masses at each floor. In particular, the first plan consisted of wooden and reinforced concrete plates with different coverings, wood and mosaic, respectively. Therefore, the masses due to self-weight of the plates and their coverings were not symmetrically distributed. The arrangement of the vertical structural members (walls) was indeed symmetric. However, the arrangement in the horizontal planes was not.

The reliability of a numerical model is usually investigated by comparing corresponding outcomes via experiments. In particular, the fundamental eigenfrequencies are usually defined by the application of Ambient Vibration Testing [10]. Therefore, the numerical model can be validated and structural characteristics as well as boundary conditions can

be identified [44]. However, this kind of experimental investigation could not be afforded by the absence of budget of the present study. Nevertheless, numerical models can sometimes be calibrated by analytical results or vice versa, under the condition that the same assumptions exist for both methods applied.

Under these premises, Table 3 presents a series of formulas used for the estimation of the fundamental eigenperiod,  $T_f$  of the masonry structures and the corresponding resulting value referred to the present study. It can be noticed that all the formulas provided the fundamental eigenperiod as function of the structural height,  $H$ . However, the Spanish Norm (NCSE-2002) [45] provides a relation which takes into account the length of the structure. Furthermore, ASCE07-16 [46], NTC-2008 [47] and EN 1998 [48] use a similar multiplier of the height's function (0.0448 and 0.05).

**Table 3.** Analytical estimation of the fundamental eigenperiod.

Reference	Formula $T_f$ [sec]	Value [sec]
ASCE 07-16 [45]	$0.0488 \cdot H^{3/4}$	0.3127
Catulo [49]	$0.03 \cdot H^{3/4}$	0.1922
NTC-2008 [46]	$0.05 \cdot H^{3/4}$	0.3204
EN 1998 [47]	$0.05 \cdot H^{3/4}$	0.3204
NCSE-2002 [44]	$0.06 \cdot H \cdot \sqrt{\frac{H}{2L+H}}$	0.1244
Calvi [48]	$\frac{\sqrt{L}}{0.04} \cdot H^{3/4}$	0.2563

Calvi [49] proposed a reduced value of the multiplier (0.04), based on the observation that masonry structures present considerable stiffness before the damage state. Furthermore, Catulo [50] proposed a reduction of the multiplier (0.03), referring to corner or isolated buildings. The fundamental eigenperiod of the studied structure according to the numerical results was estimated at 0.184 s. This outcome diverged from the results of the American, Italian, European norms and Calvi [49]. On the contrary, the fundamental numerical eigenperiod was in between the results of Catulo [50] and the Spanish norm [45]. The differences could be attributed to the assumptions that issue in each case. Although the geometry of the studied building could be considered as a typical masonry structure, the uneven distribution of stiffness (concrete and wooden plates) at the floor levels was a non-typical characteristic.

### 3.4.2. Actions and Ultimate Limit Design Situations

The permanent and variable actions were based on the information gathered regarding the structural materials and on EN 1991 [51], whereas the seismic action was based on EN 1998 [48] and the Greek National Annex to EN 1998 [52]. Table 4 summarizes the values of the permanent and variable actions.

**Table 4.** Values of the permanent and variable actions.

	Action	Value
Permanent	Masonry self-weight	25 [kN/m <sup>3</sup> ]
	Concrete self-weight	25 [kN/m <sup>3</sup> ]
	Wooden floor self-weight	8 [kN/m <sup>3</sup> ]
	Mosaic floor self-weight	1.8 [kN/m <sup>2</sup> ]
	Wooden roof trusses	0.3 [kN/m <sup>2</sup> ]
	French type tiles	0.5 [kN/m <sup>2</sup> ]
	Plasterboard	0.085 [kN/m <sup>2</sup> ]
Variable	Student congregation, furniture, etc.	3.5 [kN/m <sup>2</sup> ]
	Snow	0.625 [kN/m <sup>2</sup> ]
	Wind	0.648 [kN/m <sup>2</sup> ]

Figure 11 depicts the design spectrum used for the elastic spectral analysis. The design ground acceleration of type A ground was equal to  $a_g = 0.24 \cdot g$ , according to the seismic zone of the area. The ground type of the area corresponded to B and therefore the following values were taken into account:  $S = 1.2$ ,  $T_B = 0.15$  [s],  $T_C = 0.5$  [s],  $T_D = 2.5$  [s]. The lower bound factor for the horizontal design spectrum was equal to  $\beta = 0.2$  and the behavior factor to  $q = 1.5$ .

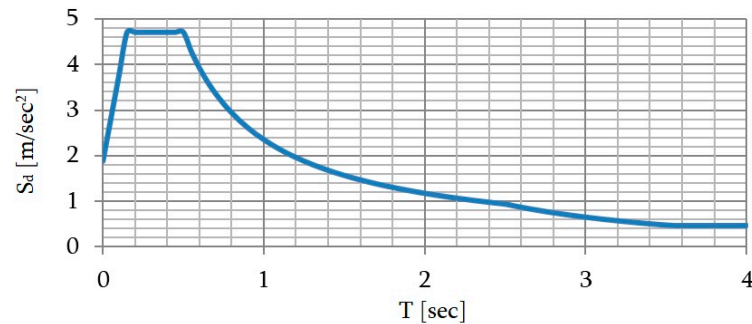


Figure 11. Design spectrum.

The two ultimate limit state (ULS) design situations that were taken into account, according to EN 1990 [53], concerned the persistent design situation and the seismic design situation. Equations (2) and (3) describe the appropriate combination of actions for each design situation.

$$\sum \gamma_{G,j} \cdot G''_{k,j} + \sum \gamma_{Q,1} \cdot Q''_{k,1} + \sum \gamma_{Q,i} \cdot \psi_{0,i} \cdot Q_{k,i}, \quad (2)$$

$$\sum G''_{k,j} + A''_{ED} + \sum \psi_{2,i} \cdot Q_{k,i} \quad (3)$$

where:

$G, Q, A$ : the permanent, variable and seismic actions, respectively;

$\psi_0 \cdot Q_k$ : the combinations value of a variable action;

$\psi_2 \cdot Q_k$ : the quasi-permanent value of a variable action;

$\gamma_G, \gamma_Q$ : the partial factors corresponding to the permanent and variable actions, respectively.

The 13 loading combinations applied to the masonry structure are depicted in Table 5.

Table 5. Loading combinations for ultimate limit state (ULS) design situations.

Design Situation	Load Combination
Persistent	$1.35 \cdot G + 1.5 \cdot Q$
	$1.35 \cdot G + 1.5 \cdot Q + 1.5 \cdot 0.6 \text{ wind}$
	$1.35 \cdot G + 1.5 \cdot Q + 1.5 \cdot 0.5 \text{ snow}$
	$1.35 \cdot G + 1.5 \cdot Q + \text{wind} + \text{snow}$
	$G + 0.6Q$
Seismic	$G + 0.6Q \pm EX \pm 0.3 \cdot EY$
	$G + 0.6Q \pm 0.3 \cdot EX \pm EY$

### 3.4.3. Persistent and Seismic Design Situations

Figure 12 depicts the deformed shape of the masonry structure, for which the maximum values of vertical stresses ( $s_{22}$ ) and shear stresses ( $s_{12}$ ) were developed during the persistent design situations. For all the examined cases, the developed stresses were less than the corresponding characteristic strength values.

The following refer to the basic outcomes of the response-spectrum analysis, which was performed by implementing mode-superposition [54]. Figure 13 depicts the deformed shape of the masonry structure, for which the maximum values of the vertical ( $s_{22}$ ) and shear stresses ( $s_{12}$ ) were developed during the seismic design situations. The results were indicative and referred to the extreme maximum stress values. The depiction of the extreme

minimum stress values was omitted. Furthermore, the non-simultaneous values of the stresses are depicted due to the conduction of the dynamic spectral analysis. The main target was the investigation of the most vulnerable zones due to seismic action. It is noted that the bearing capacity and the overall structural efficiency should be conducted on the cross-section level. The maximum vertical stress was denoted for the loading combinations  $G + 0.6 \cdot Q + 0.3 \cdot EX \pm Y$ , while the maximum shear stress for  $G + 0.6 \cdot Q - 0.3 \cdot EX - Y$ . Therefore, the significance of the seismic component, which was perpendicular to the elongated building's axis (direction Y), was designated.

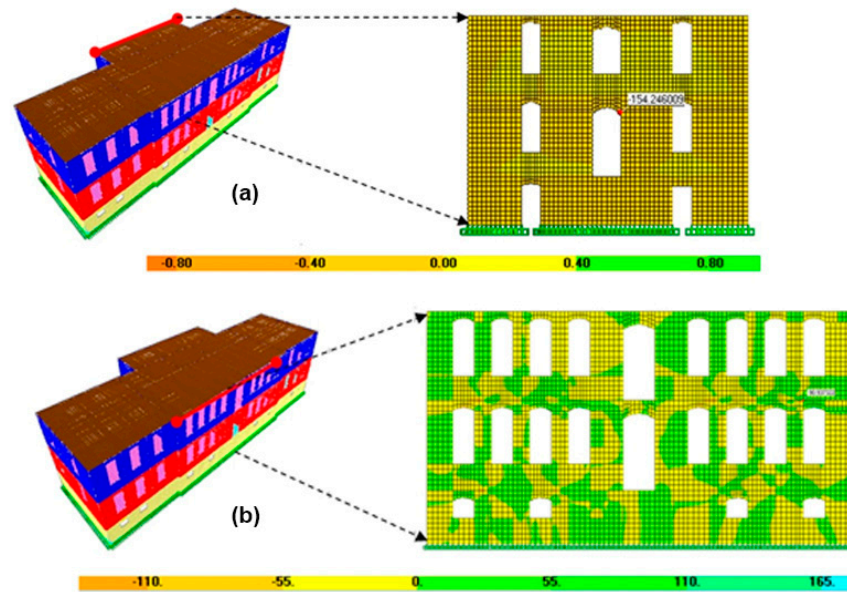


**Figure 12.** Persistent design situations. Loading combination:  $1.35 \cdot G + 1.5 \cdot Q + 1.5 \cdot 0.5 \text{ snow}$ ; (a)  $\max(s_{22}) = -154.260 \text{ KPa}$ ; (b)  $\max(s_{12}) = 90.937 \text{ KPa}$ .

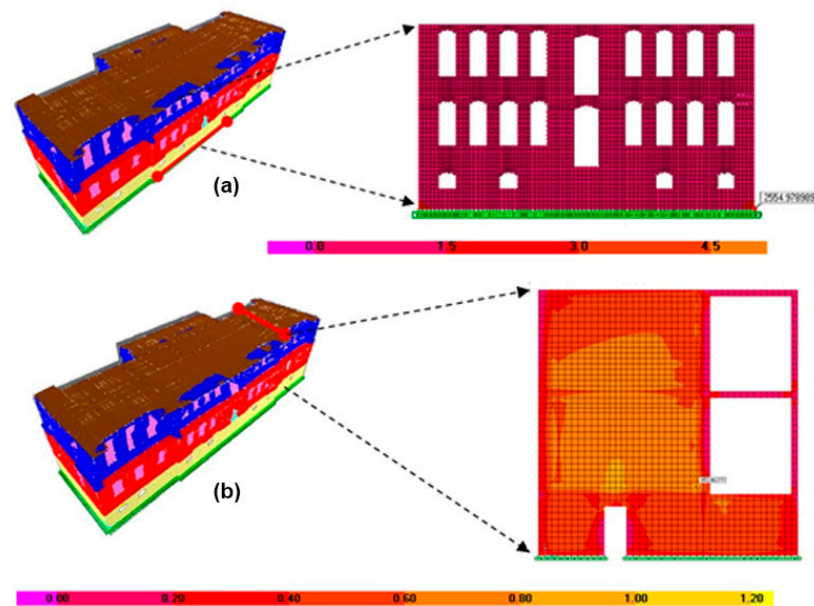


**Figure 13.** Seismic design situations: (a) Loading combination:  $G + 0.6 \cdot Q + 0.3 \cdot EX \pm Y$   $\max(s_{22}) = 2254.979 \text{ kPa}$ ; (b) Loading combination:  $G + 0.6 \cdot Q - 0.3 \cdot EX - Y$   $\max(s_{12}) = 853.803 \text{ kPa}$ .

Table 6 presents the maximum vertical ( $s_{22}$ ) and shear ( $s_{12}$ ) stresses for all the loading combinations that were investigated. It is noted that for the seismic load combinations the aforementioned values corresponded to the extreme maximum values.

**Table 6.** Maximum vertical and shear stresses for ultimate limit state (ULS) design situations.

Design Situation	Load Combination	max( $s_{22}$ ) [kPa]	max( $s_{12}$ ) [kPa]
Persistent	$1.35 \cdot G + 1.5 \cdot Q$	−122.271	60.958
	$1.35 \cdot G + 1.5 \cdot Q + 1.5 \cdot 0.6wind$	−101.647	56.281
	$1.35 \cdot G + 1.5 \cdot Q + 1.5 \cdot 0.5snow$	−154.260	90.937
	$1.35 \cdot G + 1.5 \cdot Q + wind + snow$	−101.540	67.964
Seismic	$G + 0.6 \cdot Q + EX + 0.3 \cdot Y$	1454.238	529.324
	$G + 0.6 \cdot Q - EX - 0.3 \cdot Y$	1620.110	474.579
	$G + 0.6 \cdot Q + EX - 0.3 \cdot Y$	1068.433	556.174
	$G + 0.6 \cdot Q - EX + 0.3 \cdot Y$	1620.110	524.016
	$G + 0.6 \cdot Q + 0.3 \cdot EX + Y$	2554.979	492.370
	$G + 0.6 \cdot Q + 0.3 \cdot EX - Y$	2554.979	536.110
	$G + 0.6 \cdot Q - 0.3 \cdot EX + Y$	1645.447	338.09
	$G + 0.6 \cdot Q - 0.3 \cdot EX - Y$	2554.979	853.803

The partial factor,  $\gamma_M$  for masonry under limit state situations and in particular under persistent design situations, received the value of 2.7 according to EN 1996 [39]. According to the Greek National Annex [52], the partial factor,  $\gamma_M$  under seismic design situations was reduced by 2/3, receiving the value of 1.8. Therefore, the design compressive strength became  $f_{kd,p} = 1.663$  MPa under persistent state and  $f_{kd,s} = 2.494$  MPa under seismic state situations. All the compressive stress values referring to the persistent design state received values lower than the compressive strength.

Under seismic state situations the values of compressive stresses, regarding the load combinations  $G+0.6 \cdot Q+0.3 \cdot EX \pm Y$  and  $G+0.6 \cdot Q-0.3 \cdot EX - Y$ , were close to the value of compressive strength. Furthermore, the design characteristic initial shear strength became  $f_{vko,p} = 0.037$  MPa under persistent state and  $f_{vko,p} = 0.056$  MPa under seismic state situations. All the shear stress values referring to the persistent design state received values lower than the initial shear strength. However, under seismic state situations the values of shear stresses were greater than  $f_{vko,p}$ .

In order to clarify the seismic safety under shear stresses the contribution of compressive stresses must be taken into account. Although the seismic safety assessment was not the target of the present state, since it was limited solely to the detection of the most vulnerable zones and taking into account the excellent current building state, it was deduced that limit state referring to shear stresses would possibly be fulfilled. Last and most important is the fact that for the estimation of the structural capacity under persistent or seismic loading conditions, the limit state evaluation must be fulfilled in the cross-section level, piers and spandrels by definition of the developing internal forces.

Summarizing the outcomes of the numerical analyses the following were pointed out. In the first level, the load bearing capacity of the masonry structure was verified under the persistent design situations. In the second level, the modal analysis revealed that the fundamental eigenmode corresponded to a translational mode, perpendicular to the elongated axis of the structure. The second eigenmode corresponded to a torsional mode and the third one to a translational mode, parallel to the elongated axis of the structure. In the third level, the seismic design situations revealed that the most unfavorable excitation corresponded perpendicular to the elongated axis of the structure, taking into account the values of the developed vertical and shear stresses.

#### 4. Conclusions

The studied historic school building of Arnaia revealed an abundance of qualitative information regarding its historical, architectural, constructional and structural aspects. It comprised a mixed-type structure, built according to the diachronic traditional techniques and materials (stones, lime-based mortars) and the contemporary use of reinforced concrete. The ground plans were symmetrically organized according to the S–E axis, while the

inner spaces were successively developed around a longitudinal and transversal corridor, forming a cruciform. The large openings were also symmetrically arranged, ensuring natural ventilation and lighting. The internal organization was reflected in the façades, characterized by austerity and simplicity. The masonry walls were enhanced by large pillars, extended throughout the whole height of the building, while the plates were both R/C and wooden.

The construction of a simplified, three-dimensional, linear finite element model of the building contributed to the understanding of its structural behavior. The first and third mode of vibration corresponded to translation perpendicular and parallel to the elongated axis of the structure. The second mode of vibration corresponded to torsion attributed to the asymmetric distribution of masses. Therefore, even though the arrangement of the vertical structural members was considered symmetrical, the non-uniform distribution of masses at the horizontal planes was responsible for the torsional mode of vibration. Furthermore, the analysis outcomes due to the persistent design situations clearly verified the bearing capacity of the structure. Even though the seismic safety was not evaluated during the preliminary study, the analysis results under seismic design situations revealed the most crucial zones. Therefore, the implementation of linear analysis, which is sometimes underestimated, as a first stage produce important information for a second and more thorough analysis stage referring to finer meshing at vulnerable zones; application of non-linear material; conduction of non-linear time history analysis; investigation of soil-structure interaction effects.

The preservation state of the building was generally good, with limited damages concerning render detachments and some cracks in the concrete slab of the ground floor. The critical aspects (also identified by the structural assessment) were concentrated in the eastern part of the building (damaged during the 1932 earthquake), where past repair works were implemented, as well as in the walls' conjunctions.

The overall good condition of the building maybe attributed to multiple factors, such as its functional role and structural demands leading to the application of rigorous architectural and constructional principles, as well as its constant use, which has required regular repair and upgrading. Another aspect could be the social values of the building, closely connected with the citizens' everyday life. Diachronically, school buildings were landmarks of culture and knowledge for communities, which were envisaged with their preservation and protection. To this extent, relevant sectors and scientists should be involved in order to acknowledge this significant part of our built heritage and preserve the tangible and intangible values it incorporates.

**Author Contributions:** Conceptualization, V.P.; methodology, V.P. and V.T.; software, V.P., V.T. and E.M.; validation, V.P. and V.T.; formal analysis, V.P., V.T. and E.M.; investigation, V.P., V.T. and E.M.; resources, V.P., and E.M.; data curation, V.P., V.T. and E.M.; writing—original draft preparation, V.P. and V.T.; writing—review and editing, V.P. and V.T.; visualization, V.P., V.T. and E.M.; supervision, V.P. All authors have read and agreed to the published version of the manuscript.

**Funding:** This research received no external funding.

**Institutional Review Board Statement:** Not applicable.

**Informed Consent Statement:** Not applicable.

**Data Availability Statement:** Data Availability Statements in section “MDPI Research Data Policies” at <https://www.mdpi.com/ethics>.

**Acknowledgments:** The authors would like to acknowledge the contribution of various sectors for the implementation of this study. Special thanks are attributed to the municipality of Aristotelis and the mayor, as well as to the directorate of the elementary education of Chalkidiki and the director of the school, for the close collaboration and support. Acknowledgements are also attributed to the architects involved in the past study of the building and to the citizens for providing historic information and archives.

**Conflicts of Interest:** The authors declare no conflict of interest.

## References

1. Arya, A.S. *Protection of Educational Buildings Against Earthquakes, a Manual for Designers and Builders*; Unesco: Bangkok, Thailand, 1987.
2. Abreu Marques, B.; de Brito, J.; Correia, J.R. Constructive characteristics and degradation condition of Liceu Secondary Schools in Portugal. *Int. J. Archit. Herit.* **2015**, *9*, 896–911. [[CrossRef](#)]
3. Guarini, M.R.; Morano, P.; Sica, F. Historical school buildings. A multi-criteria approach for urban sustainable projects. *Sustainability* **2020**, *12*, 1076. [[CrossRef](#)]
4. Salvado, F.; Marquesde Almeida, N.; Vale, E.; Azevedo, A. Historical analysis of the economic life-cycle performance of public school buildings. *Build. Res. Inf.* **2019**, *47*, 813–832. [[CrossRef](#)]
5. Lassandro, P.; Cosola, T.; Tundo, A. School building heritage: Energy efficiency, thermal and lighting comfort evaluation via virtual tour. *Energy Procedia* **2015**, *78*, 3168–3173. [[CrossRef](#)]
6. Martinez-Molina, A.; Boarin, P.; Tort-Ausina, I.; Vivancos, J.L. Post-occupancy evaluation of a historic primary school in Spain: Comparing PMV, TSV and PD for teachers' and pupils' thermal comfort. *Build. Environ.* **2017**, *117*, 248–259. [[CrossRef](#)]
7. Carofilis, W.; Perrone, D.; O' Reilly, G.J.; Monteiro, R.; Filiatrault, A. seismic retrofit of existing school buildings in Italy: Performance evaluation and loss estimation. *Eng. Struct.* **2020**, *225*, 111243. [[CrossRef](#)]
8. Buvik, K.; Andersen, G.; Tangen, S. Ambitious renovation of a historical school building in cold climate. *Energy Procedia* **2014**, *48*, 1442–1448. [[CrossRef](#)]
9. Watters, D.M. Our catholic school: Themes and patterns in early catholic school buildings and architecture before 1872. *Innes Rev.* **2020**, *71*, 1–66. [[CrossRef](#)]
10. Perrone, D.; O' Reilly, G.J.; Monteiro, R.; Filiatrault, A. Assessing seismic risk in typical Italian school buildings: From in-situ survey to loss estimation. *Int. J. Disaster Risk Reduct.* **2019**, *44*. [[CrossRef](#)]
11. Khledj, S.; Bencheikh, H. Impact of a retrofitting project on thermal comfort and energy efficiency of a historic school in Miliana, Algeria. *Int. J. Archit. Herit.* **2019**. [[CrossRef](#)]
12. Francois, L. *The Right to Education from Proclamation to Achievement 1948–1968*; Unipub, Inc.: New York, NY, USA, 1968.
13. Freeman, K.J. *Schools of Hellas: An Essay on the Practice and Theory of Ancient Greek Education from 600 to 300*; Rendall, M.J., Ed.; Macmillan and Co Limited: London, UK, 1912.
14. Dascalaki, E.G.; Sermpezoglou, V.G. Energy performance and indoor environmental quality in Hellenic schools. *Energy Build.* **2011**, *43*, 718–727. [[CrossRef](#)]
15. Doukas, D.I.; Bruce, T. Energy Audit and renewable integration for historic buildings: The case of Craiglockhart Primary School. *Procedia. Environ. Sci.* **2017**, *38*, 77–85. [[CrossRef](#)]
16. Galimullina, A.; Korotkova, S. Adapting the Architecture of School Buildings in the Context of Humanizing the Environment. In Proceedings of the IOP Conference Series: Materials Science and Engineering, Kazan, Russia, 29 April–15 May 2020.
17. Kalafati, E. The school buildings of the elementary education 1821–1929. In *Historic Archives of Greek Youth*; General Secretariat for Youth: Athens, Greece, 1988.
18. Pantazis, C. Mass Education and Economic Development in Greece: The Educational Reform of 1929. Ph.D. Thesis, University of Ioannina, Ioannina, Greece, June 2010.
19. Lerma, C.; Mas, A.; Blasco, V. Analysis procedure of a previous planning organization: The area of the Seminary School of Corpus Christi in Valencia, Spain. *Int. J. Archit. Herit.* **2013**, *7*, 135–152. [[CrossRef](#)]
20. Kokkonis, I.P. *Summary of the Report Given to the Commission on Primary Instruction Concerning the Manual for the Mutual-Method Schools of France*; Sarazin, J., Ed.; Egina, Greece, 1831.
21. Moraitis, S. *Διδασκαλική: ή σύντομοι οδηγία περί της χρήσεως της νέας διδασκαλικής μεθόδου*. Βιβλιοθήκη του προς Διάδοσιν των Ελληνικών Γραμμάτων Συλλόγου. 45, Σύλλογος προς Διάδοσιν των Ελληνικών Γραμμάτων. Vlastou Editions: Athens, Greece, 1880. (In Greek)
22. Kardamitsi-Adami, M.D. *Kallias and the School Building*; National Technical University of Athens: Athens, Greece, 1986.
23. Karantinos, P. *The New School Buildings*; Technical Chamber of Greece: Athens, Greece, 1938.
24. Pachta, V.; Papayianni, I. The study of the historic buildings of eclecticism in Thessaloniki under the prism of sustainability. *Procedia Environ. Sci.* **2017**, *38*, 274–282. [[CrossRef](#)]
25. Pachta, V.; Papayianni, I. Natural and Anthropogenic Hazards and Sustainable Preservation. In *10th International Symposium on the Conservation of Monuments in the Mediterranean Basin, Natural and Anthropogenic Hazards and Sustainable Preservation*; Springer: Berlin/Heidelberg, Germany, 2019; pp. 407–413.
26. Papayianni, I.; Pachta, V.; Milosi, A. The survey of a historical building from the beginning of the previous century. Evaluation of mechanical characteristics of the load bearing system. In Proceedings of the 6th International Conference on Concrete Repair, Thessaloniki, Greece, 20–23 June 2016; pp. 353–360.
27. Debailleux, L. Schmidt hammer rebound hardness tests for the characterization of ancient fired claybricks. *Int. J. Archit. Herit.* **2019**, *13*, 288–297. [[CrossRef](#)]
28. Hübllová, S.; Cikrle, P.; Karel, O.; Kocáb, D. Experimental Measurement of the Diameter and Cover Depth of Steel Reinforcement using an Electromagnetic Concrete Cover Meter. In Proceedings of the IOP Conference Series: Materials Science and Engineering, Zuberec, Slovakia, 29–31 May 2019.
29. Pavlides, S.B.; Tranos, M.D. Structural characteristics of two strong earthquakes in the North Aegean: Ierissos (1932) and Agios Efstratios (1968). *J. Struct. Geol.* **1991**, *13*, 205–214. [[CrossRef](#)]

30. Pachta, V.; Papayianni, I. Design and application of a data system for the comparative study of historic mortars. In *Lecture Notes in Computer Science (Including subseries Lecture Notes in Artificial Intelligence and Lecture Notes in Bioinformatics)*; Ioannides, M., Ed.; Springer: Berlin/Heidelberg, Germany, 2016; pp. 701–710.
31. American Concrete Institute. *1R-03 (2003): In-Place Methods to Estimate Concrete Strength*; American Concrete Institute: Indianapolis, IN, USA, 2003.
32. Castellazzi, G.; D'Altri, A.M.; de Miranda, S.; Ubertini, F. An innovative numerical modeling strategy for the structural analysis of historical monumental buildings. *Eng. Struct.* **2017**, *132*, 229–248. [[CrossRef](#)]
33. Terzi, G.V.; Ignatakis, E.C. Non linear finite element analyses for the restoration study of Xana, Greece. *Eng. Struct.* **2018**, *167*, 96–107. [[CrossRef](#)]
34. Betti, M.; Vingoli, A. Numerical assessment of the static and seismic behavior of the basilica of Santa Maria all' Impruneta (Italy). *Constr. Build. Mater.* **2011**, *25*, 4308–4324. [[CrossRef](#)]
35. Kita, A.; Cavalagli, N.; Masciotta, M.G.; Lourenço, P.B.; Ubertini, F. Rapid post-earthquake damage localization and quantification in masonry structures through multi dimensional non-linear seismic IDA. *Eng. Struct.* **2020**, *219*. [[CrossRef](#)]
36. Bartoli, G.; Betti, M.; Marra, A.M.; Monchetti, S. On the role played by the openings on the first frequency of historic masonry towers. *Bull. Earthq. Eng.* **2020**, *18*, 427–451. [[CrossRef](#)]
37. Wilson, A. Seismic Assessment of Timber Floor Diaphragms in Unreinforced Masonry Buildings. Ph.D. Thesis, The University of Auckland, Auckland, New Zealand, 2012.
38. Denskovska, L.; Aleksovski, G.; Milkova, K.; Perunkovski, K. The influence of in-plane stiffness of timber floors on the seismic response of existing masonry buildings. In Proceedings of the 16th European Conference on Earthquake Engineering, Thessaloniki, Greece, 15–21 June 2018.
39. European Committee for Standardization EN 1996-1. *Eurocode 6: Design of Masonry Structures—Part 1-1: General Rules for Reinforced and Unreinforced Masonry Structures*; European Committee for Standardization: Brussels, Belgium, 2005.
40. De Angelis, A.; Pecce, M. Seismic non structural vulnerability assessment in school buildings. *Nat. Hazards* **2015**, *79*, 1333–1358. [[CrossRef](#)]
41. Napolitano, R.; Hess, M.; Glisic, B. Integrating non-destructive testing, laser scanning, and numerical modeling for damage assessment: The Room of the Elements. *Heritage* **2019**, *2*, 151–168. [[CrossRef](#)]
42. SAP2000 v.11. Computers and Structures, Inc.: Berkeley, CA, USA, 2007. Available online: <https://adicean.mystrikingly.com/blog/sap-2000-advanced-v11-0-4-full-version-download> (accessed on 25 December 2020).
43. Marseglia, P.S.; Micelli, F.; Aiello, M.A. Analysis of equivalent diaphragm vault structures in masonry construction under horizontal forces. *Heritage* **2020**, *3*, 989–1107. [[CrossRef](#)]
44. Manolis, G.D.; Makarios, T.K.; Terzi, V.; Karetsou, I. Mode shape identification of an existing three-story flexible steel stairway as a continuous dynamic system. *Theor. Appl. Mech.* **2015**, *42*, 151–166. [[CrossRef](#)]
45. Ministerio de Fomento. *Norma de Construcción Sismorresistente: Parte General y Edificación (NCSE 02)*; Ministerio de Fomento: Madrid, Spain, 2002.
46. ASCE 07-16. *Minimum Design Loads and Associated Criteria for Buildings and Other Structures*; American Society of Civil Engineers: Virginia, VA, USA, 2017.
47. NTC-2008. Norme Tecniche per le Costruzioni. *Official Gazette of the Italian Republic*, 17 January 2018; N42.
48. European Committee for Standardization EN 1998-1. *Eurocode 8: Design of Structures for Earthquake Resistance—Part 1: General Rules, Seismic Actions and Rules for Buildings*; European Committee for Standardization: Brussels, Belgium, 2004.
49. Calvi, G. A displacement based approach for vulnerability evaluation of classes of buildings. *J. Earth. Eng.* **1999**, *3*, 411–438. [[CrossRef](#)]
50. Catulo, R. *Análise Dinâmica Experimental de Edifícios de Alvenaria e Avaliação Sísmica de um Edifício Tipo*. Ph.D. Thesis, Técnico Lisboa, Lisboa, Portugal, November 2015.
51. The European Union. *EN 1991: Eurocode 1-Actions on Structures*; The European Union: Maastricht, The Netherlands, 2002.
52. Hellenic Organization for Standardization. Greek National Annex to EN 1998-1. In *Eurocode 8: Design of Structures for Earthquake Resistance—Part 1: General Rules, Seismic Actions and Rules for Buildings*; Hellenic Organization for Standardization: Athens, Greece, 2005.
53. European Committee for Standardization EN 1990. *Eurocode—Basis of Structural Design*; European Committee for Standardization: Brussels, Belgium, 2002.
54. Wilson, E.L.; Button, M.R. Three-dimensional dynamic analysis for multi-component earthquake spectra. *Earthq. Eng. Struct. Dyn.* **1982**, *10*, 471–476. [[CrossRef](#)]